2009

Partial Ion Yield Sspectroscopy around the Cl 2p and C 1s Ionization Thresholds in CF3Cl

D. Ceolin
Uppsala University

Maria Novella Piancastelli
Uppsala University, maria-novella.piancastelli@physics.uu.se

Wayne C. Stolte
University of Nevada, Las Vegas, wcstolte@lbl.gov

Dennis W. Lindle
University of Nevada, Las Vegas, lindle@unlv.nevada.edu

Partial ion yield spectroscopy around the Cl 2p and C 1s ionization thresholds in CF3Cl

D. Céolin, M. N. Piancastelli, W. C. Stolte, and D. W. Lindle

Citation: J. Chem. Phys. **131**, 244301 (2009); doi: 10.1063/1.3274642
View online: http://dx.doi.org/10.1063/1.3274642
View Table of Contents: http://jcp.aip.org/resource/1/JCPSA6/v131/i24
Published by the American Institute of Physics.

Partial ion yield spectroscopy around the Cl 2p and C 1s ionization thresholds in CF_3Cl

D. Céolin,[1,a] M. N. Piancastelli,[1] W. C. Stolte,[2] and D. W. Lindle[2]
[1]*Department of Physics and Materials Science, Uppsala University, P.O. Box 530, SE-751 21 Uppsala, Sweden*
[2]*Department of Chemistry, University of Nevada, Las Vegas, Nevada 89154-4003, USA*

(Received 14 September 2009; accepted 24 November 2009; published online 22 December 2009)

We present a partial ion yield experiment on freon 13, CF_3Cl, excited in the vicinity of the C 1s and Cl 2p ionization thresholds. We have collected a large amount of cationic fragments and a few anionic fragments at both edges. We have observed a strong intensity dependence of Rydberg transitions with ion fragment size for the CF_nCl^+ and CF_n^+/F^+ (n=0–3) series at both the Cl 2p and C 1s ionization edges. Selectivity in the fragmentation processes involving the C–Cl and C–F bonds are highlighted by the intensities of the C 1s to lowest unoccupied molecular orbital (LUMO) and LUMO+1 transitions measured on the CF_nCl^+ and CF_n^+ yields. Equally, by comparison with their cation counterpart, we discuss possible bond-length dependence for the anion formation at the carbon 1s edge. © *2009 American Institute of Physics*. [doi:10.1063/1.3274642]

I. INTRODUCTION

The chloro-fluoro carbons known as freons play an important role in several atmospheric chemical reactions.[1] They have been widely used in industry, for example, as refrigerants, foam blowing agents, aerosol propellants, and for plasma etching processes commonly used in semiconductor fabrication.[2] However, it is now widely recognized that these compounds are responsible, via photochemical mechanisms, for the depletion of the Earth's ozone layer in the stratosphere.[3] Thus there is applied as well as fundamental interest in obtaining spectroscopic information for freons in the far UV and soft x-ray regions of the electromagnetic spectrum corresponding to the energetic solar radiation present in the upper levels of the Earth's atmosphere,[4] in particular in what concerns their electronic structure and dynamic properties in photoexcitation and decay events.

Several different spectroscopic techniques have been used to characterize the interaction between freons and ultraviolet or x-ray radiation. Examples include inner-shell x-ray absorption[5–8] and x-ray emission,[9] inner-shell electron energy loss,[10–12] valence photoelectron spectroscopy,[13,14] Auger spectroscopy,[15] and partial ion yield spectroscopy.[16] *Ab initio* calculations of core-excitation spectra have also been reported.[17]

In the present work we will concentrate on partial ion yield experiments, where we collect one mass-selected positive or negative ion as a function of photon energy in an interval usually including one or more ionization thresholds. The underlying physics is the following: after the creation of a core hole by an incident photon in a molecule, valence electrons, which form the chemical bonds, are ejected via the dominating Auger process, and the molecule usually dissociates into fragments, ions, and/or neutrals. In order to understand such photofragmentation processes in more detail, it is useful to consider the regions below and above the ionization threshold separately. Below the threshold, following the excitation of a core electron to a bound unoccupied molecular orbital, a core hole decays via resonant Auger processes either by participator or spectator decay.[18,19] After resonant Auger decay, which typically produces singly ionized states, the molecule is often unstable and dissociates into small ionic or neutral fragments. Above the ionization threshold, normal Auger decay dominates, yielding a doubly charged ion that is even more likely to dissociate.

Compared to photoabsorption or absorptionlike measurements, such as total electron or total ion yield (TIY) (including near-edge x-ray absorption fine structure for gas-phase and adsorbed species), there is a clear advantage in monitoring a channel that is highly selective with respect to different types of resonances. Moreover, our experimental apparatus possesses the unique capability to detect either positively charged species (cation) or negatively charged species (anions). Partial anion yield is more selective than other single-channel measurements. Recently, we have applied anion-yield spectroscopy to a number of small molecules, and it has proven to be a selective probe of molecular core-level processes, e.g., providing unique experimental verification of shape resonances[20–22] and identifying specific bond-breaking processes in methanol.[23]

Another interesting finding derived from partial ion yield spectroscopy is the assessment that below threshold, the relative intensity for spectral features related to core-to-Rydberg excitation increases as the fragmentation process is more extended. In other words, for the lighter fragments, the Rydberg states are much more prominent than for the parent molecular ions. This is directly related to spectator decay being

[a]Present address: Division of Synchrotron Radiation Research, Lund University, Box 118—SE-221 00 Lund, Sweden. Author to whom correspondence should be addressed. Electronic mail: denis.ceolin@sljus.lu.se.

much more probable following excitation to the diffuse Rydberg orbitals, and many or most of the final two-hole/one-particle states are dissociative.[24,25]

A longstanding debate in the literature concerns the possibility of site-selective fragmentation following Auger decay. The best known example of site-selective fragmentation concerns halogen-substituted hydrocarbons;[26] therefore another reason to investigate freons is to assess the relative importance of such processes. Site-selective fragmentation was reported in the $CF_\alpha Cl_{4-\alpha}$ series above the Cl 2p and F 1s ionization thresholds by previous comparatively low-resolution ion yield experiments.[16]

We report here a detailed study of fragmentation processes around the Cl 2p and C 1s ionization thresholds in one of the prototypical freons, CF_3Cl. Beside studying a chlorofluoro system, we also intended to compare the photofragmentation pathways for CF_3Cl with those of another molecule we have previously investigated, CH_3Cl,[25] to elucidate the influence of replacing hydrogen with fluorine on the photofragmentation dynamics. We have obtained partial ion yields for all detectable positive and negative fragments with state-of-the art experimental resolution. Above the Cl 2p threshold, we detect a large amount of Cl^+ but also a comparable amount of F^+. The formation of these two ions can be followed by monitoring the photon energy, and strong variations are seen in the ratio Cl^+/F^+ as a function of the excitation energy. Therefore we do not observe strong site selectivity as it is conclude in Ref. 16. We attribute the difference to the higher sensitivity of our spectrometer, especially to the fact that we are able to estimate the ratio between resonant and nonresonant processes on a large photon energy scale.

We observe a relatively higher intensity of the spectral features related to transitions to Rydberg states in the anion yields, which we attribute to an extended fragmentation taking place in the final states reached after spectator decay. Furthermore, we observe that continuum features attributed to shape resonances are barely visible in the anion yield curves, confirming our previous observation that anion production in the shape resonance region is reduced, since anions should stem from the fragmentation of positively doubly charged species resulting from Auger decay.

At the Cl 2p edges we observe that extended fragmentation is also evident in the cation yields upon transitions to Rydberg states. This effect is not clearly evident at the C 1s edge, where spectator decay seems to play an important role also for transitions to virtual molecular orbitals.

We find evidence for selective C–Cl bond breaking and possibly ultrafast dissociation leading directly to the formation of the CF_3^+ fragment upon excitation from the C 1s core level to the lowest unoccupied molecular orbital (LUMO) ($11a_1$ virtual orbital with antibonding character along the C–Cl bond). In a similar way, the strong intensity of the CF_2Cl^+ fragment at the photon energy related to the transition C 1s to the second and third unoccupied orbitals confirms the very dissociative character along the C–F bond of the corresponding intermediate state.

II. EXPERIMENT

Experiments were performed on beamline 8.0.1.3 at the Advanced Light Source, Lawrence Berkeley National Laboratory. The monochromator calibration near the chlorine 2p and carbon 1s edges was performed by comparison to the high-resolution photoabsorption measurements by Zhang *et al.*[10] Ion mass and charge characterization was done with a 180° magnetic mass analyzer with a resolution of 1 mass in 50.[27] Briefly, the fragments are created by interaction with the light beam at the exit of an effusive gas jet. Ions are extracted from the gas cell by an electric field and focused on the entrance slit of the analyzer by an electrostatic lens. They are then deflected between the poles of the analyzer and refocused onto the exit slit before being detected by a channel electron multiplier. The potentials of the analyzer can be tuned and/or switched in polarity to select fragments with a specific mass and charge. The working pressure in the target chamber was approximately 1×10^{-5} Torr, and the chamber was isolated from the beamline vacuum by differential pumping. The CF_3Cl, freon 13, was obtained commercially during the late 1990s from DuPont de Nemours and Co., with a stated purity 100%, and introduced in the vacuum chamber without further purification.

III. RESULTS AND DISCUSSION

The symmetry point group of CF_3Cl is C_{3v} and its electronic structure in an independent particle picture are the following:[10] $1a_1^2$ (Cl 1s) $2a_1^2$ $1e^4$ (F 1s) $3a_1^2$ (C 1s) $4a_1^2$ (Cl 2s) $5a_1^2$ $2e^4$ (Cl 2p) for the inner shells and $6a_1^2$ $3e^4$ $7a_1^2$ $8a_1^2$ $4e^4$ $9a_1^2$ $5e^4$ $6e^4$ $1a_2^2$ $10a_1^2$ $7e^4$ $11a_1^0$ $8e^0$ $12a_1^0$ for the valence shells. The lowest-lying unoccupied orbitals correspond to levels with antibonding character along the C–Cl bond (a_1 symmetry), antibonding character along the C–F bond (e symmetry) and antibonding character along the C–F bond (a_1 symmetry), respectively.

We have obtained total and partial ion yields for all detectable ionic fragments in the photon energy range 190–335 eV, including the Cl 2p and C 1s ionization thresholds at 207.83 eV (Cl $2p_{3/2}$), 209.44 eV (Cl $2p_{1/2}$), and 300.31 eV (C 1s).[10] The energy calibration has been performed according to Ref. 10. The singly charged positive fragments (cations) are the following: CF_3Cl^+, CF_2Cl^+, $CFCl^+$, CCl^+, CF_3^+, CF_2^+, CF^+, C^+, F^+, Cl^+, plus the recombination fragments ClF^+ and F_2^+. The doubly or multiply charged positive fragments are CF_2Cl^{++}, $CFCl^{++}$, CF_2^{++}, CF^{++}, CCl^{++}, and C^{++}. The negatively charged species (anions) are C^-, F^-, and Cl^-.

We show the TIY in Fig. 1. The Cl 2p and C 1s ionization thresholds are also shown. The interpretation of the spectral features is the following:[10] the peaks at 201.13 and 202.71 eV correspond to the transitions from the two spin-orbit split Cl 2p levels to the $11a_1$ LUMO with an antibonding character along the C–Cl bond; the peaks at 204.31 and 205.84 eV account for the transitions from the Cl 2p levels to the $8e+12a_1$ virtual orbitals, plus the contribution of the 4p Rydberg level converging to the Cl $2p_{3/2}$ threshold to the structure at 205.84 eV; the peaks at 206.26 and 206.36 eV correspond to transitions from the Cl $2p_{3/2}$ to the 5s, 5p

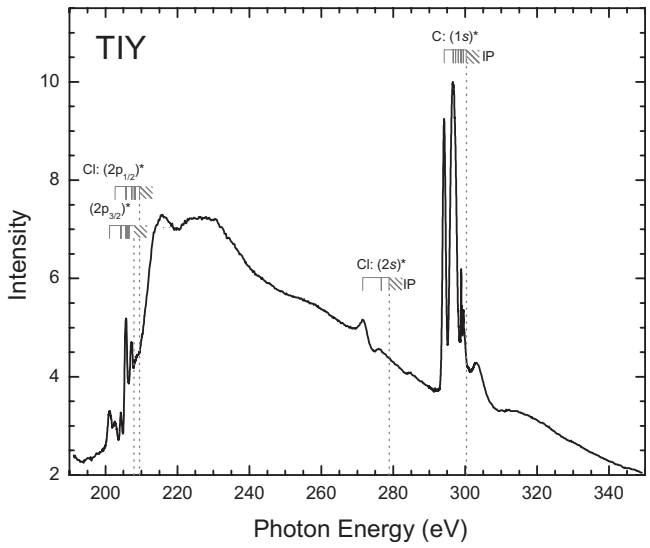

FIG. 1. TIY taken over a large photon energy range including the Cl 2p, Cl 2s, and C 1s ionization thresholds.

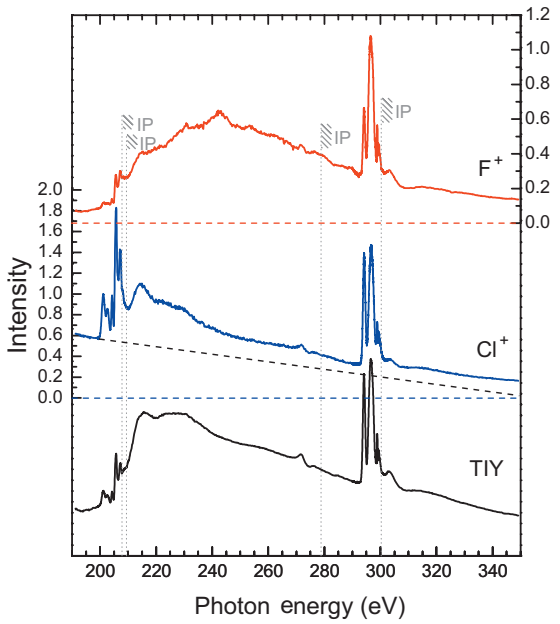

FIG. 2. F^+ and Cl^+ partial yields compared with the TIY. The red and blue horizontal dashed lines correspond to the zero baselines of F^+ and Cl^+, respectively. The black dashed line corresponds to the estimated valence shells photoionization contribution of the Cl^+ yield. The scales on the left and right axes correspond to the Cl^+ and F^+ yields, respectively. The two partial ion yields are normalized with each other but are not normalized with the TIY. The ionization potentials IPs mentioned in Fig. 1 are also reported.

Rydberg levels; the peak at 207.32 eV corresponds to the Cl $2p_{1/2} \rightarrow 4p$ resonance; the thresholds for the Cl $2p_{3/2}$ and $2p_{1/2}$ are respectively at 207.83 and 209.44 eV; the above-threshold broad features at 215 and 228 eV correspond to shape resonances; the peak at 271.50 eV accounts for the Cl $2s \rightarrow$ LUMO transition; the Cl 2s threshold is at 278.84 eV; the peaks at 294.16, 296.66, and 297.30 eV correspond to transitions from the C 1s level to the first three virtual orbitals, followed by peaks at 298.07, 298.82, 298.93, and 299.46 eV accounting respectively for the transitions from the C 1s level to the 4p, 5s, 5p, and 6s Rydberg levels; the C 1s threshold is located at 300.31 eV; and finally the broad features above threshold at 303.12 and 318 eV correspond to shape resonances.

While we rely on literature results for the interpretation of the spectral features, the main interest of our experiments stems from the comparison between the TIY, mimicking photoabsorption, and the partial ion yields of the various different fragments. We will discuss in the following sections in great detail the two more significant spectral regions including the Cl 2p and the C 1s ionization thresholds. Here we begin with some general consideration on the overall appearance of our yield curves for some of the fragments.

In Fig. 2 we report the partial ion yields for Cl^+ and F^+ over the whole range investigated. A direct comparison between the yields of these two ions was mentioned in Ref. 16. The authors detected F^+ with significantly less abundance than Cl^+ above the Cl 2p ionization thresholds. Therefore they concluded that the normal Auger decay following Cl 2p ionization leads to final states with two positive charges, which are localized around the chlorine atom, and the subsequent fragmentation favors the rupture of the C–Cl bond, with emission of Cl^+, but not that one of the C–F bond(s). In other words, site-selective fragmentation was observed for CF_3Cl.

Site-selective fragmentation, implying that an ion fragment is produced at the same molecular site where the primary excitation has taken place is a sought-after effect in the literature. To be able to cut a specific chemical bond by creating a core hole on one specific atom in a polyatomic molecule would be an extremely interesting possibility with a series of practical applications. However, the selectivity in the excitation process is not sufficient condition to ensure selectivity in photofragmentation, and the details of excitation-de-excitation processes need to be taken into account. In particular, the degree of localization of the Auger process following core excitation or ionization plays a key role. The electronic relaxation process can be described in a two-step model: photoelectron emission followed by a normal Auger process leading to a doubly charged ion. A site-specific dissociation process of this doubly charged ion can then be forecasted only if the location of the two positive charges in the final two-hole state of the Auger process is around the initial core-hole site. This is frequently the case since the Auger decay rate depends on the overlap between the core-hole orbital and the molecular orbitals participating in the Auger process.

At variance with Ref. 16, our finding contradicts the occurrence of high selectivity in the Auger decay of the Cl 2p core-hole states. First, we notice that the overall appearance of the F^+ yield above threshold depends on the photon energy and is different in shape from the Cl^+ one, in particular far above the Cl 2p edges. We attribute this difference to the presence of a shape resonance and to the opening of double ionization and satellite thresholds. Then, we are able to estimate the background contribution due to direct valence photoionization processes in the formation of these two ions. The background observed on the Cl^+ yield is significantly decreasing with the photon energy, whereas it is not the case for the F^+ fragment. For instance, regarding the Cl^+ frag-

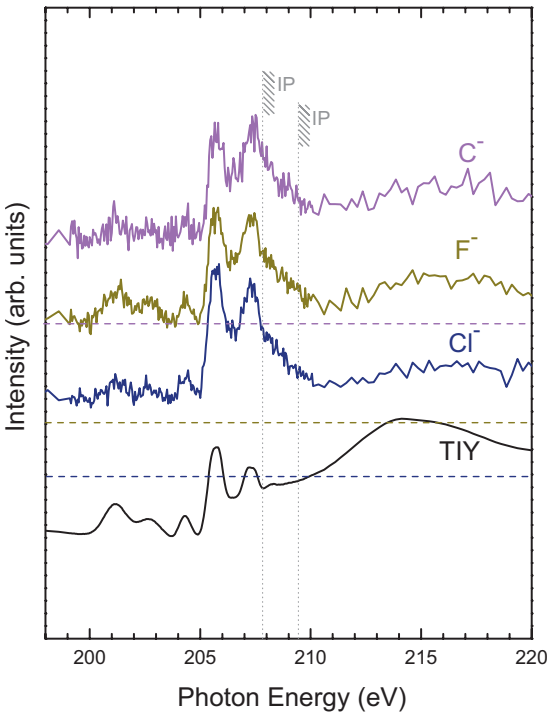

FIG. 3. C^-, F^-, and Cl^- partial yields compared with the TIY taken in the vicinity of the Cl 2p thresholds. The horizontal dashed lines correspond to the zero baselines.

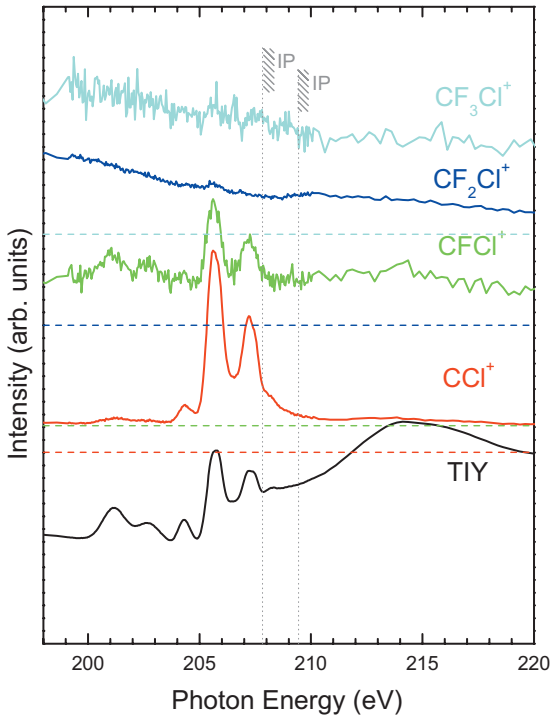

FIG. 4. Partial yields of the CF_iCl^+ (i=0–3) series compared with the TIY taken in the vicinity of the Cl 2p thresholds. The horizontal dashed lines correspond to the zero baselines. The curves, which are not normalized to each other, illustrate qualitatively the intensity increase of the Rydberg series as compared with the valence series while the fragment size decreases.

ment, the background at about 215 eV photon energy represents about one-half of the total intensity, whereas it represents less than one quarter in the F^+ case. This valence contribution taken into account, the F^+ and Cl^+ yield are about the same. At higher photon energy, the Cl^+ formation yield decreases—background contribution subtracted—whereas the one of F^+ is increasing. For example, at 240 eV photon energy, the F^+ formation processes involving core orbitals are obviously more efficient than the Cl^+ ones. After subtraction of the valence shell photoionization contributions, we estimate the formation of F^+ to be two times larger than the one of Cl^+. However, we remark a selective effect on the Cl^+ formation below the Cl 2p thresholds, on resonance, especially at photon energies corresponding to the transitions to Rydberg orbitals.

A. CF_3Cl: Cl 2p edge

In Fig. 3 we report the anion yields in the photon energy range including the Cl 2p thresholds together with the TIY for sake of comparison. As a general remark, we notice that anion production is more abundant in correspondence of discrete below-threshold resonances and is reduced above the ionization thresholds. Another observation is that the features corresponding to transitions to Rydberg states are more pronounced in the anion yields than in the TIY. This finding can be explained by the nature of the resonant Auger decay following excitation to Rydberg states: the main pathway is spectator decay leading to final states which fragment more easily than the one reached after participator decay, and therefore more pathways are possible, including more leading to anion production.

Furthermore, the broad features corresponding to shape resonances visible in the TIY are comparatively very weak in the anion yields. This behavior can be rationalized by observing that the decay pattern for the discrete resonances is resonant Auger decay, leading to final states with one electron vacancy, which can fragment producing positive and negative ions, while above threshold normal Auger decay takes place, leading to final states with two electron vacancies whose fragmentation to produce negative ions is much less likely. In particular, we observe that shape resonances show very little or almost no intensity in the anion curves, in accordance with observations we previously reported in other systems.[20–22] In the F^- yield the shape resonance features are slightly more evident, but this can be attributed to electron capture by the electronegative F atom more than to fragmentation leading directly to F^- species.

In Fig. 4 we show the partial ion yields for the series CF_3Cl^+, CF_2Cl^+, $CFCl^+$, and CCl^+, which we can consider a sequential breaking of C–F bonds. We observe that the relative intensity of the parent ion is quite low, indicating that it is not stable upon photoionization. The other yields show an effect we have already described in several cases. Namely, we notice that the relative intensity of the spectral features related to transitions to the Rydberg series (see above discussion for the spectral assignment) increases steadily while compared to the structures related to transitions to empty molecular orbitals. This effect has been reported by us in several other systems (see, e.g., Refs. 24 and 25), and it is explained by the nature of the final states reached after resonant Auger decay from core-excited states where the excited electron is promoted to a virtual orbital or to a Rydberg or-

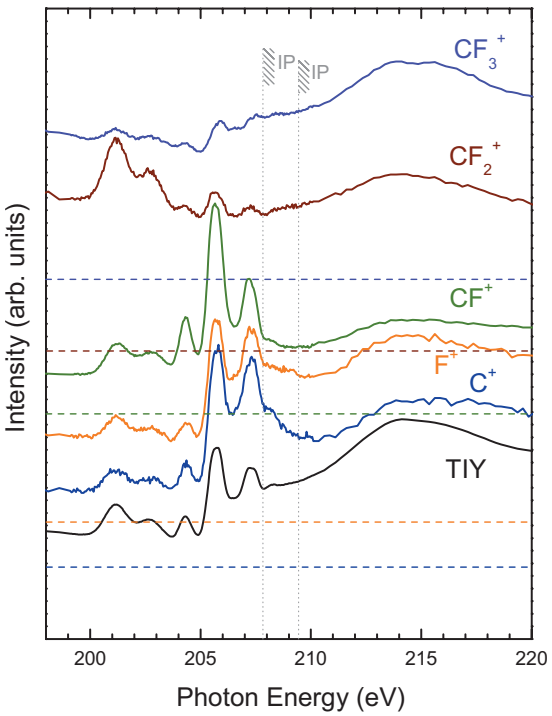

FIG. 5. Partial yields of the CF_i^+ (i=0–3) series and F^+ compared with the TIY taken in the vicinity of the Cl 2p thresholds. The horizontal dashed lines correspond to the zero baselines. The curves, which are not normalized to each other, illustrate qualitatively the intensity increase of the Rydberg series as compared with the valence series while the fragment size decreases.

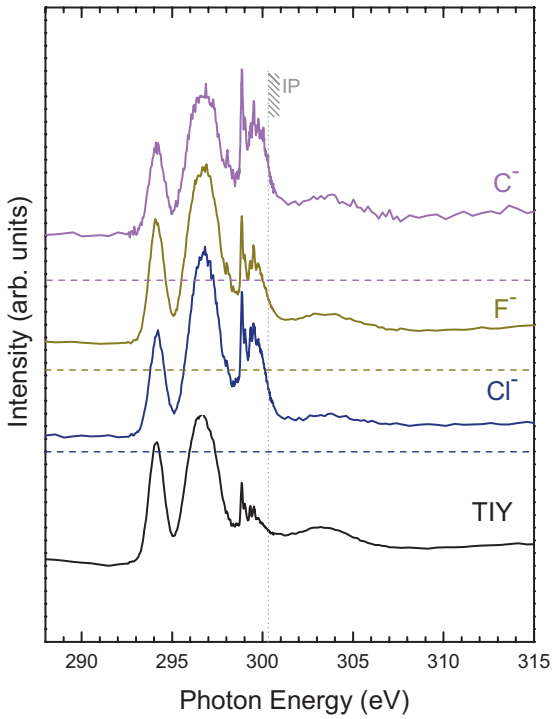

FIG. 6. C^-, F^- and Cl^- partial yields compared with the TIY taken in the vicinity of the C 1s threshold. The horizontal dashed lines correspond to the zero baselines.

bital, respectively. In the first case, the majority of decay processes is categorized as participator decay, leading to relatively long-lived one-hole valence final states, while when the primary excitation involves Rydberg states, the system with one electron in an orbital far from the ionic core relaxes preferentially by spectator Auger decay and the singly charged ion with two valence holes and one electron on an outer diffuse orbital remains in excited states more susceptible to dissociate. The same effect can be noticed if we compare the fragments CF_3^+, CF_2^+, CF^+, C^+, and F^+, shown in Fig. 5.

The yields of the doubly and multiply charged cations (not shown) have the common characteristics of showing an enhanced edge jump at the ionization thresholds, linked to the production of species with two valence electron vacancies resulting from normal Auger decay.

B. CF_3Cl: C 1s edge

In Fig. 6 we show the anion yields in the photon energy region including the C 1s ionization threshold. The same considerations reported above for the Cl 2p thresholds hold: anion production is more abundant in correspondence of discrete below-threshold resonances and is reduced above the ionization thresholds; the features corresponding to transitions to Rydberg states are more pronounced in the anion yields than in the TIY; the broad features corresponding to shape resonances visible in the TIY are comparatively weaker in the anion yields.

The ion yields of most positive fragments in the energy region including the C 1s ionization threshold mimic the TIY, therefore not showing evidence for specific pathways leading to one particular fragment. A very significant exception is the CF_x^+ series yields, shown in Fig. 7 together with the TIY for sake of comparison. It is evident that the relative

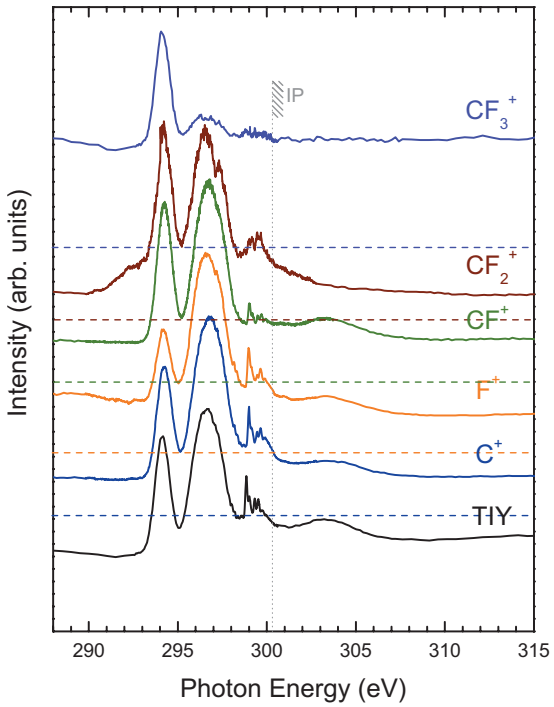

FIG. 7. Partial yields of the CF_i^+ (i=0–3) series and F^+ compared with the TIY taken in the vicinity of the C 1s threshold. The horizontal dashed lines correspond to the zero baselines. The curves, which are not normalized to each other, illustrate qualitatively the intensity increase of the Rydberg series as compared with the valence series while the fragment size decreases.

intensity of the peak at 294.16 eV is much higher in the CF_3^+ yield compared to the TIY. Similar effects to a lower extent are also visible in the CF_2^+ and CF^+ curves.

This peak is assigned to the $C1s \rightarrow 11a_1$ transition, where the virtual orbital has an antibonding character along the C–Cl bond. Its relative intensity in all the CF_x^+ curves suggests that the excitation to this intermediate state is followed by decay to final states with electron vacancies located around the C–Cl bond, which then is broken easily. Therefore we observe a selective fragmentation process. A similar effect was reported for CH_3Cl,[25] where the yields of CH_x^+ fragments showed enhanced intensity in correspondence to the transition from the C 1s level to the LUMO, again suggesting a selective C–Cl bond-breaking process.

In the present case, we notice that the effect is much stronger for the CF_3^+ fragment, hinting at an additional channel for its production. We suggest the following interpretation: when an electron is promoted from a core level to a virtual orbital, if the latter is dissociative in nature a phenomenon called ultrafast dissociation can occur. Namely, the core-excited neutral state can dissociate before resonant Auger decay, and the electron decay then takes place in the fragment where the core hole is located. If the dissociation takes place on the same timescale as the electron decay (usually few femtoseconds depending on the depth of the core hole and the natural lifetime of the core-excited state), then it is labeled ultrafast. The first example of the occurrence of such event was described for HBr,[28] and since then many other examples have been reported (see, e.g., Refs. 29–32).

In CF_3Cl, the occurrence of ultrafast dissociation following the $C1s \rightarrow 11a_1$ transition would imply the rupture of the C–Cl bond before electron relaxation and subsequently the resonant Auger decay in the CF_3 neutral fragment, where the core hole induced by the primary excitation is located. This would explain the "anomalous" intensity of the spectral feature related to the $C1s \rightarrow 11a_1$ transition in the CF_3^+ yield: ultrafast dissociation would imply an extra channel for this fragment, which would be in part produced directly after electron decay and would not only be the result of a second-step process such as fragmentation following Auger decay.

In Fig. 8 we show the yields for the series CF_3Cl^+, CF_2Cl^+, $CFCl^+$, and CCl^+. For the corresponding results at the Cl 2p edges, shown in Fig. 4, we have noticed that the peaks related to the Rydberg series increase in intensity as a function of the extent of fragmentation and explained on the ground of dominant spectator decay following transitions to Rydberg states. In the present case, this trend is not evident, but we notice the increase in intensity of the feature related to the transition to the LUMO as a function of fragmentation. Since we connect this effect to the decay to dissociative final states, more likely to be reached after spectator decay, we conclude that in this case either spectator decay is also relevant following the decay of the excitation to the LUMO, or some of the final states reached after participator decay are dissociative in nature. This latter hypothesis is consistent with the observation that the parent ion is detected with very low intensity, and therefore the majority of final states reached after electron decay should lead to easy fragmentation.

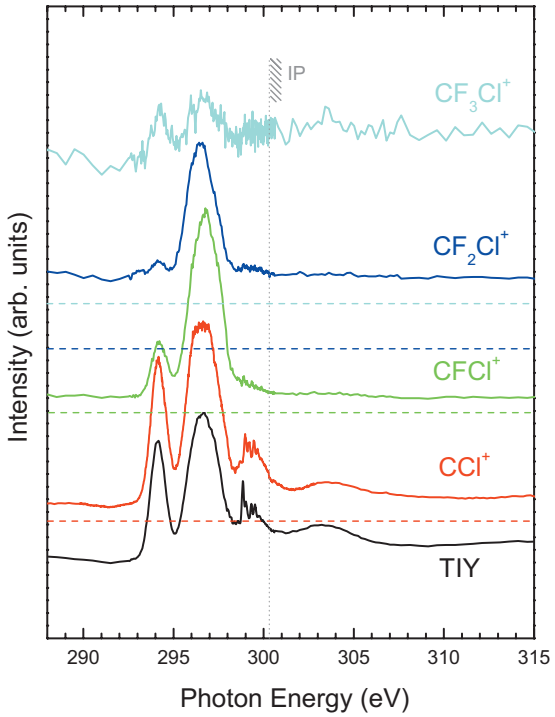

FIG. 8. Partial yields of the CF_iCl^+ (i=0–3) series compared with the TIY taken in the vicinity of the C 1s threshold. The horizontal dashed lines correspond to the zero baselines. The curves, which are not normalized to each other, illustrate qualitatively the intensity increase of the Rydberg series as compared with the valence series while the fragment size decreases.

In Fig. 9 we compare the anion yields of Cl^-, F^-, and C^- with the cation yields of Cl^+, F^+, and C^+, respectively. A clear shift in the $C1s \rightarrow 11a_1$ and $C1s \rightarrow 8e+12a_1$ resonances maxima is observed for the Cl^- and F^- yields as compared with the Cl^+ and F^+ ones. This shift is almost absent in the C^-/C^+ case. A similar behavior was observed on CH_3Cl where the Cl^- formation appeared to be less intense than the Cl^+ yield for the low photon energy side of the first resonance.[25] This was attributed to the repulsive character of the core-excited state and to the photoexcitation process, which preferentially reaches the Franck–Condon region corresponding to longer (shorter) bonds distances at lower (higher) photon energies along the profile of this strongly antibonding resonance. This effect was suggesting a possible bond-length dependence in the formation of anionic species. In the present case we repeat this interpretation for the two first resonances, the first one being repulsive mainly along the C–Cl bond as interpreted from the CF_3^+ yield, and the second one being repulsive mainly along a C–F bond as interpreted from the CF_2Cl^+ yield. However, it is important to note that, for instance, in the Cl^+/Cl^- yields comparison, a shift in the $C1s \rightarrow 8e+12a_1$ resonance position is also observed. It would mean that this bond is not fully describable by orbitals located only along C–F but that a C–Cl character has to be taken into account. A similar reasoning can be applied to interpret the shift observed on the first resonance when we compare the F^+/F^- yields. In Addition, the fact that we do not observe a clear shift in the C^- yield is explained by a preferential location of the extra negative charge on the most electronegative fragment, i.e., on Cl when the C–Cl bond is broken and on F when C–F is broken.

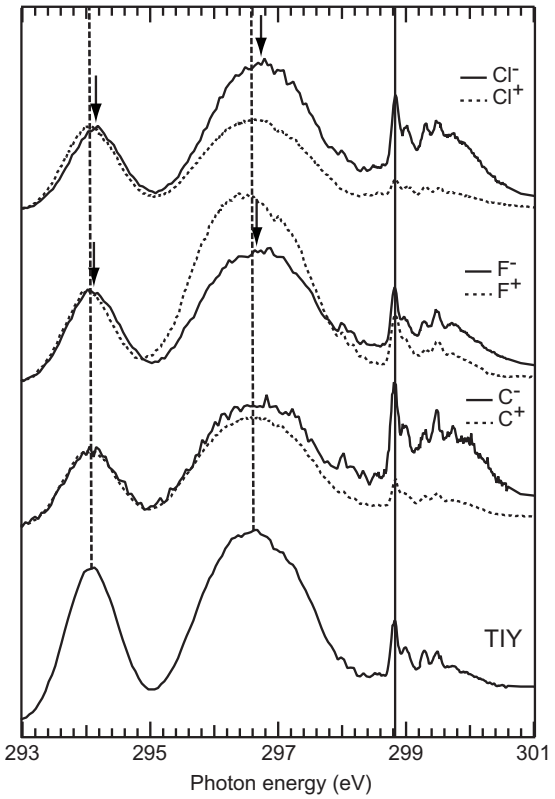

FIG. 9. Partial ion yields of the anions Cl^-, F^- and C^- fragments in the vicinity of the C 1s ionization threshold. These spectra are compared to partial ion yields of Cl^+, F^+, and C^+ to the TIY and are calibrated in energy on the first Rydberg component. They are normalized on the maximum intensity of the first resonance. The vertical dashed lines indicate the maximum positions of the two first resonances on the TIY, and the arrows indicate the maximum position of the first two resonances on the Cl^- and F^- anion yields. All of them are shifted to the high photon energy side as compared with the corresponding Cl^+ and F^+ yields. An interpretation of these shifts is given in the text.

IV. CONCLUSION

In the present study we have strengthened several general interpretations concerning the fragmentation of core-excited species, highlighted in previous studies using the total and partial ion yield spectroscopy technique. Namely, on CF_3Cl core-excited/ionized in the vicinity of the C 1s and Cl 2p thresholds, we confirm the role of the transition to Rydberg orbitals in the formation of lighter fragment species, a production of anion more abundant below than above thresholds, and a possible bond-length dependence on the Cl^- and F^- formation. We have also highlighted selective fragmentation at the C 1s edge on the first and second resonance, but we have not evidenced a particularly strong selectivity above the Cl 2p edge.

ACKNOWLEDGMENTS

The authors thank the staff of the ALS, especially G. Ackerman, for their excellent support. Support from the National Science Foundation under NSF Grant No. PHY-05-55699 is gratefully acknowledged. M.N.P. thanks the Wenner-Gren Stiftelse for a grant to support her stay at the ALS. This work was performed at the Advanced Light Source, which is supported by DOE (Grant No. DE-AC03-76SF00098).

[1] *Chlorofluoromethanes and the Stratosphere*, in NASA Reference Publication 1010, edited by R. D. Hudson (National Aeronautics and Space Administration, Washington, D.C., 1977).
[2] *Plasma Reactions and Their Applications*, Japan Materials Report (Japan Technical Information Service, ASM International, Metals Park, OH, 1988).
[3] M. J. Molm and F. S. Rowland, Rev. Geophys. Space Phys. **13**, 1 (1975).
[4] H. Massey and A. E. Potten, *Atmospheric Chemistry*, Royal Institute of Chemistry Lecture Series, Vol. 1 (Royal Institute of Chemistry, London, 1961) pp. 1–27.
[5] M. J. Hanus and E. Gilberg, J. Phys. B **9**, 137 (1976).
[6] B. E. Cole and R. N. Dexter, J. Quant. Spectrosc. Radiat. Transf. **19**, 303 (1978).
[7] G. O'Sullivan, J. Phys. B **15**, 2385 (1982).
[8] C. T. Chen and F. Sette, Phys. Scr., T **3**, 119 (1990).
[9] R. C. C. Perera, P. L. Cowan, D. W. Lindle, R. E. LaVilla, T. Jach, and R. D. Deslattes, Phys. Rev. A **43**, 3609 (1991).
[10] W. Zhang, T. Ibuki, and C. E. Brion, Chem. Phys. **160**, 435 (1992).
[11] J. F. Ying and K. T. Leung, J. Chem. Phys. **101**, 7311 (1994).
[12] K. T. Leung, J. Electron Spectrosc. Relat. Phenom. **100**, 237 (1999).
[13] G. Cooper, W. Zhang, and C. E. Brion, Chem. Phys. **145**, 117 (1990).
[14] J. Doucet, P. Sauvageau, and C. Sandorfy, J. Chem. Phys. **58**, 3708 (1973).
[15] Y. Shimizu, K. Ueda, H. Chiba, M. Okunishi, K. Ohmori, Y. Sato, I. H. Suzuki, T. Ibuki, and K. Okada, Chem. Phys. **244**, 439 (1999).
[16] I. H. Suzuki, N. Saito, and J. D. Bozek, J. Electron Spectrosc. Relat. Phenom. **101–103**, 69 (1999).
[17] G. Fronzoni and P. Decleva, Chem. Phys. **237**, 21 (1998).
[18] J. Kikuma and B. P. Tonner, J. Electron Spectrosc. Relat. Phenom. **82**, 41 (1996).
[19] S.-Y. Chen, C.-I. Ma, D. M. Hanson, K. Lee, and D. Y. Kim, J. Electron Spectrosc. Relat. Phenom. **93**, 61 (1998).
[20] W. C. Stolte, D. L. Hansen, M. N. Piancastelli, I. Dominguez Lopez, A. Rizvi, O. Hemmers, H. Wang, A. S. Schlachter, M. S. Lubell, and D. W. Lindle, Phys. Rev. Lett. **86**, 4504 (2001).
[21] D. L. Hansen, W. C. Stolte, O. Hemmers, R. Guillemin, and D. W. Lindle, J. Phys. B **35**, L381 (2002).
[22] G. Öhrwall, M. M. Sant'Anna, W. C. Stolte, I. Dominguez Lopez, L. T. N. Dang, A. S. Schlachter, and D. W. Lindle, J. Phys. B **35**, 4543 (2002).
[23] W. C. Stolte, G. Öhrwall, M. M. Sant'Anna, I. Dominguez Lopez, L. T. N. Dang, M. N. Piancastelli, and D. W. Lindle, J. Phys. B **35**, L253 (2002).
[24] M. N. Piancastelli, W. C. Stolte, G. Öhrwall, S.-W. Yu, D. Bull, K. Lantz, A. S. Schlachter, and D. W. Lindle, J. Chem. Phys. **117**, 8264 (2002).
[25] D. Céolin, M. N. Piancastelli, R. Guillemin, W. C. Stolte, S.-W. Yu, O. Hemmers, and D. W. Lindle, J. Chem. Phys. **126**, 084309 (2007).
[26] C. Miron, M. Simon, N. Leclercq, D. L. Hansen, and P. Morin, Phys. Rev. Lett. **81**, 4104 (1998).
[27] W. C. Stolte, R. Guillemin, S.-W. Yu, and D. W. Lindle, J. Phys. B **41**, 145102 (2008).
[28] P. Morin and I. Nenner, Phys. Rev. Lett. **56**, 1913 (1986).
[29] O. Björneholm, M. Bässler, I. Hjelte, R. Feifel, H. Wang, C. Miron, M. N. Piancastelli, S. Svensson, S. L. Sorensen, F. Gel'mukhanov, and H. Ågren, Phys. Rev. Lett. **84**, 2826 (2000).
[30] I. Hjelte, M. N. Piancastelli, R. F. Fink, O. Björneholm, M. Bässler, R. Feifel, A. Giertz, H. Wang, K. Wiesner, A. Ausmees, C. Miron, S. L. Sorensen, and S. Svensson, Chem. Phys. Lett. **334**, 151 (2001).
[31] I. Hjelte, M. N. Piancastelli, C. M. Jansson, K. Wiesner, O. Björneholm, M. Bässler, S. L. Sorensen, and S. Svensson, Chem. Phys. Lett. **370**, 781 (2003).
[32] R. Feifel, F. Burmeister, P. Salek, M. N. Piancastelli, M. Bässler, S. L. Sorensen, C. Miron, H. Wang, I. Hjelte, O. Björneholm, A. Naves de Brito, F. Gel'mukhanov, H. Ågren, and S. Svensson, Phys. Rev. Lett. **85**, 3133 (2000).